

T. KLEKIEL*[#], R. BĘDZIŃSKI*

FINITE ELEMENT ANALYSIS OF LARGE DEFORMATION OF ARTICULAR CARTILAGE IN UPPER ANKLE JOINT OF OCCUPANT IN MILITARY VEHICLES DURING EXPLOSION

ANALIZA METODĄ ELEMENTÓW SKOŃCZONYCH DUŻYCH ODKSZTAŁCENI CHRZĄSTKI STAWOWEJ W GÓRNEJ CZĘŚCI STAWU SKOKOWEGO PASAŻERA W WOJSKOWYM POJEŹDZIE PODCZAS WYBUCHU

The paper presents the analysis of the load of lower limbs of occupants in the armoured military vehicle, which has been destroyed by detonation of the Improvised Explosive Device (IED) charge under the vehicle. A simplified model of the human lower limb focused on upper ankle joint was developed in order to determine the reaction forces in joints and load in particular segments during the blast load. The model of upper ankle joint, include a tibia and an ankle bone with corresponding articular cartilage, has been developed. An analysis of the stress distribution under the influence of forces applied at different angles to the biomechanical axis of a limb has been performed. We analyzed the case of the lower limb of a sitting man leaning his feet on the floor. It has been shown that during a foot pronation induced by a knee outward deviation, the axial load on the foot causes significantly greater tension in the tibia. At the same time it has been shown that within the medial malleolus, tensile stresses occur on the surface of the bone which may lead to fracture of the medial malleolus. It is a common case of injuries caused by loads on foot of passengers in armored vehicles during a mine or IED load under the vehicle. It was shown that the outward deviation of the knee increases the risk of the foot injury within the ankle joint.

Keywords: Large deformation, Finite element modeling, lower limb injury, upper ankle joint, military vehicle, explosion

W artykule przedstawiono analizę MES obciążenia kończyn dolnych osób w opancerzonym pojeździe wojskowym, który został zniszczony przez zaimprovizowaną detonację ładunku wybuchowego (IED) pod pojazdem. W uproszczonym modelu dolnej kończyny ludzkiej skoncentrowano się na górnej części stawu skokowego. Model opracowany został w celu określenia siły reakcji w stawach i obciążenia w poszczególnych segmentach podczas obciążenia wybuchowego. Model górnego stawu skokowego, obejmuje kość piszczelową oraz kości stawu skokowego z odpowiadającymi chrząstkami stawowymi. Przeprowadzono analizę rozkładu naprężeń pod wpływem sił wywieranych pod różnymi kątami w stosunku do osi biomechanicznej kończyny. Przeanalizowano przypadek kończyny dolnej siedzącego mężczyzny z nogą opartą na podłodze. Wykazano, że podczas skręcenia stopy indukowanego przez odwiedzenie kolana na zewnątrz, siła osiowa na stopie powoduje znacznie większe naprężenie rozciągające w kości piszczelowej. Jednocześnie wykazano, że w kostce przyśrodkowej, naprężenia rozciągające występują na powierzchni kości, co może prowadzić do wystąpienia złamania kostki przyśrodkowej. Jest to częsty przypadek obrażeń spowodowanych obciążeniami stóp pasażerów pojazdów pancernych podczas eksplozji miny lub wybuchu ładunku (IED) pod pojazdem. Wykazano, że odchylenie kolana zwiększa ryzyko obrażeń stopy w stawie skokowym.

1. Introduction

One of the essential elements to ensure the safety of passengers in the armored vehicle is to protect them from the effects of the mines and IEDs explosion in the surrounding of the vehicle. Usually, when there is a load detonation under the vehicle, the shock wave, by moving to the vehicle construction, has influence on elements of the human body, which are in a direct contact

with vehicle elements such as a floor or a seat. Statistics show that a large part of injuries relates to the lower extremities, of which approx. 25% of all injuries are related to the ankle joint and a foot. In modern solutions of military vehicles the complex composite structures are used to absorb energy [1]. Such materials have good characteristic to absorb energy enforced by dynamic impact of the pressure from the explosion and the shock wave. It was indicated that the level of energy absorption

* UNIVERSITY OF ZIELONA GÓRA, DIVISION OF BIOMEDICAL ENGINEERING, DEPARTMENT OF MECHANICAL ENGINEERING, POLAND

Corresponding authors: t.klekiel@ibem.uz.zgora.pl

strongly depends on the load type. Apart from explosion under vehicle, many problems for safety of occupants arise during explosion from one side of vehicle [2].

From the numerical experiments it results that during the charge explosion under the vehicle the occupant body is subjected to considerable impulse loads. The analysis of the impact forces in the lower limbs showed that loads formed in the tissue of limbs mostly lead to damages in the area of the joints. This results both from the limb position while sitting and the directions of the impact forces. Analyzing the injuries statistics involving the IED charges under the vehicle, noteworthy is the fact that with small explosion forces the common injuries involve the bruises around the knee and ankle joint. This mainly results from the fact that the limb during the vehicle movement is moving involuntarily. The muscle forces of the limbs and the caused torques in the joints are not able to counteract the forces generated during the shock wave originating from the explosion and during the vertical movement of the vehicle. Thus, the occupants are not able to counteract these overloads and are exposed to injuries in contact with the elements of the vehicle equipment.

When passengers inside vehicle are subjected to the explosion located centrally under the vehicle its movement is vertical. Assuming no unsealing of the vehicle, the source of injuries of passengers will mostly include the acceleration of the vehicle and the local deformation of the structure caused by the shock wave. No considering the possibility of additional injuries caused by interior objects not attached to the vehicle structure, injuries will mostly concern the lower limbs and the spine [3]. Lower limbs in such situation will be exposed to the contact with the vehicle elements and to the shock wave resulting from the deformation of the vehicle floor.

Ankle joint is composed of three bones: the tibia, fibula and talus. These bones are interconnected with ligaments, which stabilize the joint as well as maintain the natural geometry required to transfer loads properly. From the top of the joint there is the tibia, its articular surface has a shape resembling a cone with its apex pointing medially towards to the medial ankle [4]. The shape of the articular surface shows that the radius of curvature in the transverse direction is greater than in the medial direction. Articular surface of the tibia has a key role to plantar and dorsal flexion of the foot.

Deltoid ligament stabilizes the ankle medially. The presence of this ligament is very important from the point of view of carrying loads and pressures appearing on the articular surface [5]. Group of ligaments supporting connection of the tibia and fibula consists of the anterior and posterior tibio-fibular ligament, a transverse ligament and tibio-fibular membrane. To the lateral stability of ankles contribute anterior talofibular ligament (ATFL), calcaneofibular ligament (CFL) and posterior talofibular ligament (PTFL). Location of the talus is determined by the tension of lateral ligaments. In the case of the dorsal flexion PTFL and CFL ligaments are strained, and in the case of plantar flexion – ATFL and CFL ligaments [6].

Due to the complex structure and construction of the ankle joint, the position of the feet is essential for the propagation of

strain energy. The paper presents the results of analysis of the deformation of the ankle propagation for dangerous variants of the load. That is, when at the joint – both on the articular surface and in ligaments and muscles – the maximum stresses appear, that can lead to fractures and breaking of ligaments or muscles.

The analysis of literature and data from the battlefield show that in most cases of the explosion victims, soldiers feel pain in the area of the ankle joint, unless there was an explicit dislocation of the joint or fracture in its area. This indicates that, on the one hand, the size of damages can result from the arrangement of the limb, and on the other hand, from the nature of the load. Under this point, the analysis of the loading of the ankle joint were performed in order to examine the relationship between the position of the limb and trauma, which gives us initial guidelines for a more detailed numerical analyzes for selected cases.

Construction of the upper joint in the frontal plane limits the movement of the talus relative to the tibia and fibula. Ankle joint has got one degree of freedom allowing dorsal and plantar flexion of the foot. Two bones – tibia and talus are some kind of forceps for the maintenance of the talus. Transfer of the load from the calcaneus bone to the tibia is done through the talus. Lower limb alignment relative to the basis has got a significant impact on the load distribution. Passive participation in joint stability take ligaments preventing any movement in the frontal plane.

Fracture of the medial malleolus of the tibia is usually associated with a fracture of the lateral malleolus just above or at the level of the distal tibiofibular joint. It is a “low” variety of a Dupuytren fracture. In one variant of this state in the medial malleolus fracture site, there is a tear of the medial collateral ligament. “Low” Dupuytren fracture can also be associated with a fracture of the rear edge of the tibial base, which is the third free section of a bone or constituting one block with a fragment of the medial malleolus [7].

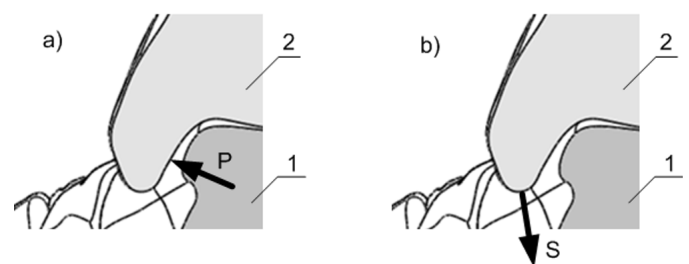


Fig. 1. Causes of the medial malleolus damage: a) the pressure of the talus on the inner part of the distal articular surface of the tibia, b) the tensile strength of the medial ligament. (1 – talus bone, 2 – tibia)

Important function for the propagation and distribution of stresses in the joint has got a cartilage, and one of its primary tasks is to evenly distribute the load on bones. Analysis of the impact of the cartilage on the load distribution is a relatively difficult issue. As we know, cartilage elasticity allows cushioning of dynamic loads. This flexibility also changes the geometry of the contact of joint surfaces. Kent et al [8] analyzed the stresses occurring in the articular cartilage of the knee. Articular surface geometry authors gained based on data obtained from MRI. In

the analysis using a finite element method, three models of a material for cartilage contact were adopted: linear, Neo-Hookean and Mooney-Rivlin. As a result similar stress values for each model with the same loads were gained, but their distribution and location of concentration were significantly different. Therefore, proper selection of material parameters is equally important, next to the geometry of joints.

2. Materials and Methods

Anatomically, the foot is one of the most complex structures with many joints and significant mobility. Foot contains 26 bones, 33 joints, 107 ligaments and 33 muscles [9]. This is approx. 25% of all human bones. These components work together to provide the body balance and mobility. Failure of one of these elements can lead to serious disturbances in the functioning of the entire limb while having a devastating impact on other segments of the body.

Contact of the foot with the ground takes place on a relatively small surface, which causes considerable forces generated during stance and walking. High loads during military march, practicing different sports act for a relatively long period of time. Foot and ankle joint is usually shaped in such a way that it can transfer so great loads. There is a different situation, when the loads are impulsive, where high energy is concentrated in a small area, eg. at the junction of articular surfaces. Most of the ongoing research works are focused on the foot and ankle joint and are related to biomechanical analyzes of the impact of tissues under static conditions [10-13] in the analysis of the processes of tissue overcharge [10,14] or the use of prosthetic and orthotic supplies [11,15].

There are few papers that relate to the conditions of the foot and footwear cooperation in the context of the analysis of load distribution. Good examples of numerical analysis using the finite element method can be work of Tian Xia Qiu et al [16] and Cho et al [17]. The effects of the interaction between the foot and the shoe in the case of impulse loads such as jumps (including jumping with a parachute) or shoes of soldiers exposed to landmines in armored vehicles, provide a basis for understanding the causes of limb injuries in the area of the ankle joint. Bischof et al [18] analyzed the contact parameters on the articular surface of the ankle joint in the case of lateral instability of the ankle joint caused by damage to the ligaments AFTL and CFL. Presented study focused on the quasi-static case. The main conclusion of the study was to demonstrate that the lateral instability of the ankle joint increases the burden on the cartilage and stress concentration coincides with the places where it was found the appearance of degenerative conditions. It must therefore be assumed that the behavior of the ligaments including the strength and material characteristics have a significant impact on the distribution of stresses on the cartilage. Thus, taking into account the impact of the ligaments have a significant impact not only on the stress concentration at selected points of the articular surface but also can affect the energy density in the case of impulse loads.

Can Xu et al [19] examined the biomechanical effects of the deltoid ligament reconstruction, which often causes pain in case of ankle joint overloads. For the analysis, the finite element method was used, containing 6 bony structures, cartilage and 9 major ligaments. The numerical model was constructed based on the MRI images. The Wei et al [20] determines the deformation forces in the ligaments. The authors used SolidWorks software with *motion* module to simulation of movements in the ankle joint. They designated in this way the forces acting in the ligaments and resistance of tissues for different positions of the foot. Authors did not take into account the fact that the bony structures are deformed during the movement which affects the tendon load. However, due to the simple uniaxial static load induced by a body weight, the influence of the deformability could be omitted. At the same time they showed a significant effect of the ligaments on the stress distribution in the joint.

To the bone structure has been given the rigid surface elements, appropriate for small deformation compared to the structure of the soft tissues. Articular cartilage is modeled using deformable elements, solid tetrahedral. For modeling ligaments linear elements has been used, which give the ability to give a preload. Placing the ligaments have been determined on the basis of their anatomical arrangement based on the literature [21]. The structure of ligaments was modeled using a single line or a group of lines depending on their geometry based on the publication [22]. Material properties were selected on the basis of literature data. Articular cartilage layer was an isotropic material $E=0.7$ MPa, $\nu = 0.49$ [23].

2.1. Computational model

In the paper an analysis of the impact of load parameters on the stress distribution in the tibia was performed. The analysis was to demonstrate the relationship between the arrangement of the limb and the tensile stress concentration around the medial malleolus.

An analysis of the medial malleolus fracture formation was based on numerical model obtained from CT imaging data of 42 y.o. man. A limb damage occurred in the armored vehicle subjected to detonation load of IED placed under the vehicle. Rupture of the medial malleolus occurred due to the load impulse from the shock wave generated by distortion of the vehicle floor during the explosion. Injury in the form of a broken medial malleolus is shown in (Fig. 2.)

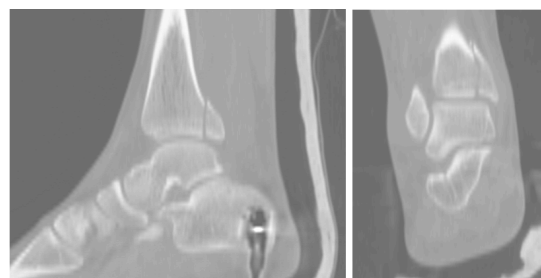


Fig. 2. CT Image of right ankle joint

Table 1 shows the values used in the calculations of the joint loading. The ankle joint loading at 5 kN is due to the fact that it is usually a lower limit of the loading [24], after which the probability of injury is one hundred percent. From the dependence no. 1 we can determine a security of the body criterion under the influence of impulse loads. The HIC Parameter (Head injury criterion) determines the probability of injury to the head under the influence of acceleration expressed with function $a(t)$.

$$HIC = \left\{ \left[\frac{1}{t_2 - t_1} \int_{t_1}^{t_2} a(t) dt \right]^{2.5} (t_2 - t_1) \right\}_{\max} \quad (1)$$

where t_1 and t_2 are the initial and final times (in seconds) of the interval during which HIC attains a maximum value, and acceleration a is measured in standard gravity acceleration. Note also the maximum time duration of HIC, $t_2 - t_1$, is limited to a specific value between 3 and 36 ms, usually 15 ms.

The force value at the level of 12 kN was adopted on the basis of literature data as the average value of the load of the tibia obtained by simulation of the shock wave propagation in the knee and experimental studies using Hybrid III [25] and cadaver limbs [26, 27].

TABLE 1

Parameters for boundary conditions

Load Force [kN]	Load direction	Reference
5	Axial	Masouros et al [24]
12	Axial	Suresh et al, [26]

A biomechanical analysis of the ankle joint shows, that damage to the medial malleolus of the tibia may occur as a result of the flow of energy from the talus on a small area of cooperation of joint elements. Another potential source of loads can be the interaction of transverse forces from the gas pressure and a shock wave. From the description of the analyzed event we can see, that during the incident there were no leaks of the vehicle hull, so the impact of the pressure and other transverse forces must be considered as marginal.

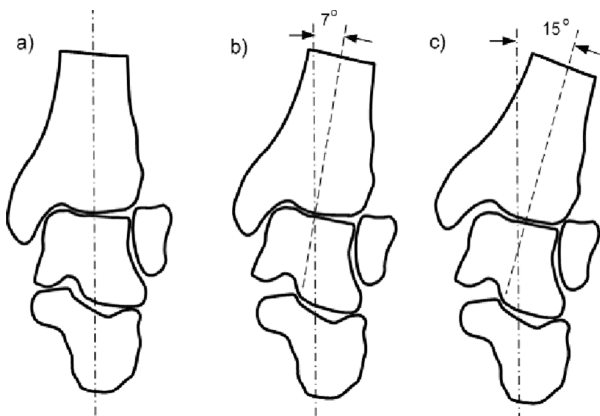


Fig 3. The position of the foot relative to the main axis of the distal extremity of the lower limb

Fig. 3 shows three analyzed cases of the position of the limb around the ankle joint. The foot abduction cases result from the alignment of the mechanical axis of the shin. This axis is the symmetry axis for the knee joint surfaces and passes through the center of the ankle joint. Case a) reflects a situation in which the person is sitting in the passenger seat with his knees together. Such an arrangement of limbs is usually rare in the armored vehicle while traveling over uneven terrain especially because of the need to occupants respond to vertical inertial forces generated during the movement of the vehicle. As a result, the more likely is the case b) or c) wherein knees are apart. We assumed two positions, where the first (7 degrees deviation) is half the mobility of the foot.

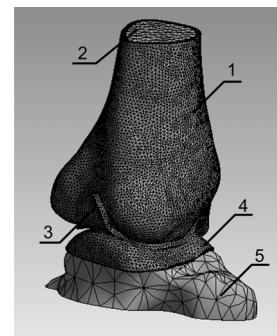


Fig. 4. Numerical model of upper ankle joint

Fig. 4 shows a model of the ankle joint which includes the tibia. It consists of cortical 1 and cancellous 2 layers. The joint surfaces 3 and 4 reflect the actual shape of the articular cartilage derived based on the MRI image. The shape and characteristics of the tibia were obtained based on the CT image. Talus (5) was assumed as a homogenous structure.

TABLE 2

Material Properties of ankle joint elements

Material	Mechanical Property	Values	Reference
Bone – homogenous	Young’s Modulus	1,00E+10	Pa Shanti and Patil [33]
	Poisson Ratio	0,34	
Cartilage	Young’s Modulus	1,00E+07	Pa Shanti and Patil [33]
	Poisson Ratio	0,4	
Trabecular Bone of Tibia	Young’s Modulus	1,06E+09	Pa Suk-Hun et al [34]
	Poisson Ratio	0,225	
Cortical Bone of Tibia	Young’s Modulus	2,14E+10	Pa Suk-Hun et al [34]
	Poisson Ratio	0,3	

At simulation studies the method of finite elements is usually used to determine both the deformability of tissues and stress in the bone structures [28, 29]. Such approach requires the use of complex discrete models of the human body and data about

material properties [30, 31]. The constitutive equations described nonlinear relation between stress and deformation for biological materials such as bones, ligaments, etc. provided to the strong nonlinear solution. The results obtained from these models are characterized much errors and limited in case of large deflection [32]. In this paper the material properties are chosen as isotropic for all elements. Table 2 shows adopted properties of biological materials, which are included in the analyzed model. The irregular characteristics of bone was included by two phase of bone strength: trabecular inside and cortical structure outside of Tibia.

3. Results

Analyzing the mechanism of fracture formation of the medial malleolus of the tibia we should pay attention to the distribution of stresses depending on the position of the shin relative to the foot. Case I (Fig. 5), in which the mechanical axis of the shin is approximately perpendicular to the ground, the axial load on the limb causes significant stress concentration on the medial malleolus. Due to forces tangential to the contact surfaces on the joint surface, there are formed both compressive and tensile stresses on the inner surface of the medial malleolus. Such stress distribution is causing presence of large gradients in different directions, which may increase the probability of injury.

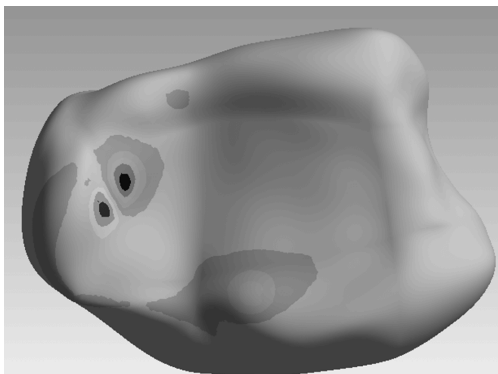


Fig. 5. Stresses for the I-st case

In the IIIrd case the outward deviation of the shin through the knee at 15 degrees, the stress analysis on the articular surface of the tibia shows, that the stress concentration is different.

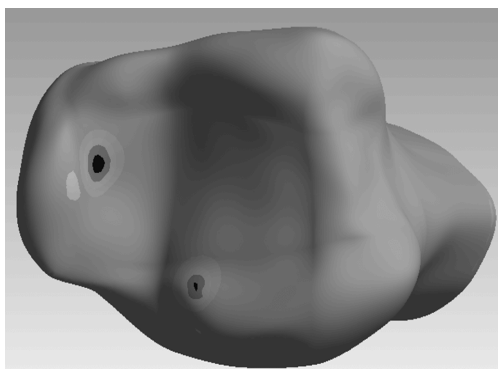


Fig. 6. Stresses for the III-rd case

The geometry of the distal tibia head indicates that the position of the limb should result in greater concentration of loads exerted on the medial malleolus. On the basis of performed calculations, it was found that the normal loads to the joint surface transmitted through the articular cartilage cause stresses distribution over a larger surface of the bone. Thus, the resulting stresses in the structure of the cortical bone are much smaller.

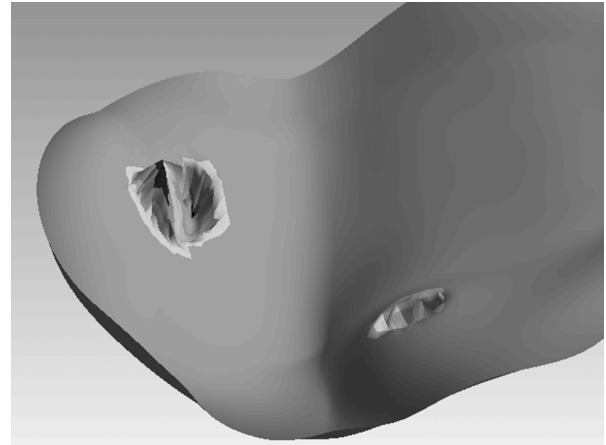


Fig. 7. Distribution of stress concentration on the surface of the articular cartilage for the case III

In the case of tangential forces transmitted to the upper ankle joint, the cartilage contact with the bone results in larger differences in stresses in the vicinity of the contact of the joint surfaces. This gives increase to the danger of cracking. At the same time, analyzing the stress distribution on the surface of the cartilage it was found that at the amount of load force of 5 kN, maximum stress levels occurring in the cartilage is approx. 360 MPa. It considerably exceeds the strength of the cartilage, which is approx. 10-15 MPa.

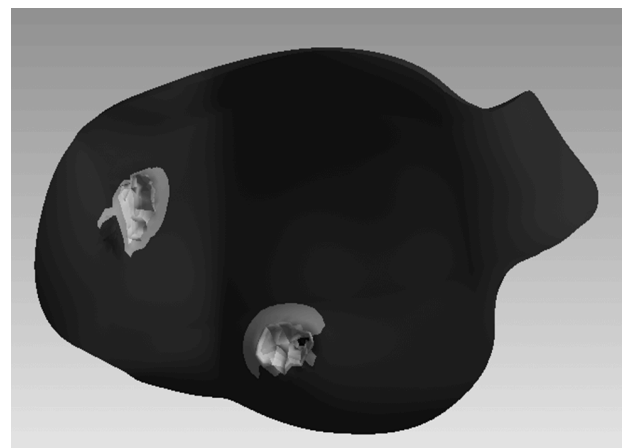


Fig. 8. Distribution of stress concentration on the surface of the articular cartilage for the case III

In the IIIrd case of the arrangement of the limb, the area of contact is slightly larger. Simultaneously, gained stresses of 55 MPa indicate a much less destructive acting of the load on the structure of the cartilage.

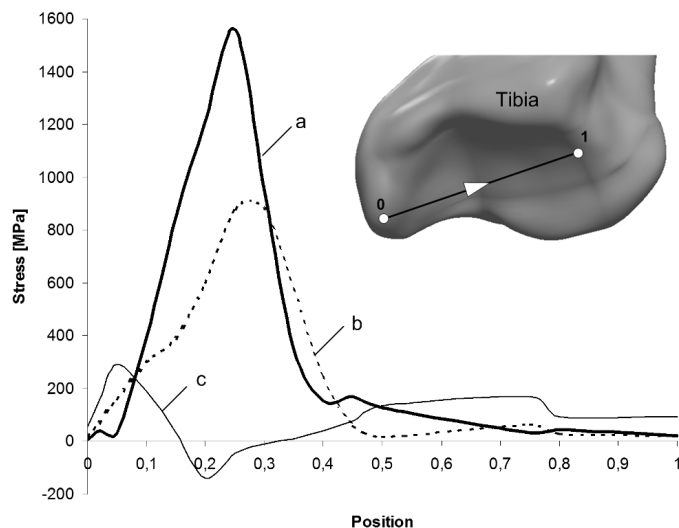


Fig. 9. The stresses along the axis of the articular surface of the tibia for the load of 5 kN

Figures 9 and 10 are made based on the measured stress along the main axis of the articular surface of the distal tibial head. Figure 9 shows the course of stresses along the axis of the articular surface of the tibia to the load of 5 kN. The curve a) shows the stresses for the case I of the feet alignment. As it is apparent from the graph the maximum stress generated on the surface of the bone was about 650 MPa. In case II, the maximum stress was 400 MPa. The smallest load was obtained for case III, in which the largest shift in the axis of the tibia relative to the vertical axis was admitted. It can be argued that with increased angle of the limb shift the stress peak moves to the center of the articular surface of the tibia.

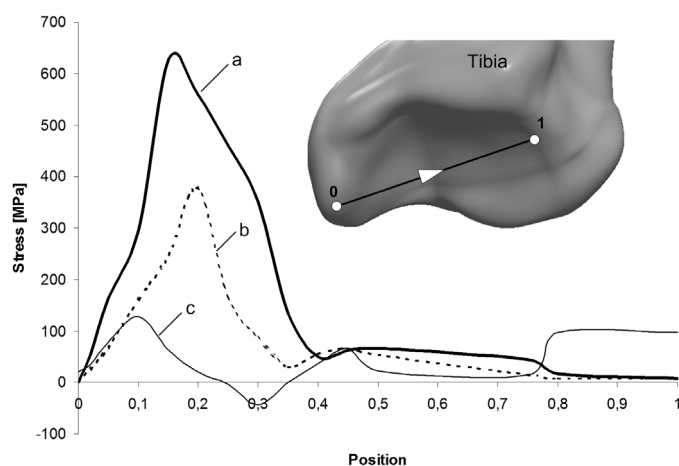


Fig. 10. The stresses along the axis of the articular surface of the tibia for the load of 12 kN

In the case of larger loads (Fig. 10) the point of maximum stress is shifted more to the center, which indicates higher deformation of cartilage caused by stresses tangent to the articular surface.

4. Conclusions

In the paper authors attempt to reproduce the conditions of formation of the medial malleolus fracture as a result of weight-bearing axial impulse force. Numerical analysis was conducted to estimate the load under the action of which a damage occurred, and to determine the effect of limb alignment to rupture the tibia. We analyzed two types of loads of ankle joint caused by forces originating from the floor, and acting on the calcaneus bone. Thus, it is assumed that the entire load is transferred to the ankle joint. We also adopted the assumption that the foot pronation occurs in the lower ankle joint and the upper joint is fully stable.

Based on gained results it can be concluded that in the case of impulse loads, the contact of articular surfaces is more punctual than superficial. The interaction between the articular surfaces takes place in a small space, which demonstrates a high stress concentration even at quite low loads.

The analysis of the stress distribution for three cases of limb positions shows, that the probability of injury is greatest when the leg is vertical to the ground. In other cases, the interaction forces directed normally to the surface of the medial malleolus reduced stress levels, there by proving that this limb arrangement is safer.

Acknowledgement

This investigation was supported by a research grant, as a part of the project DOBR-BIO/22/13149/2013: "Improvement of safety and protection of soldiers on missions through military-medical and technical operations" sponsored by the National Centre for Research and Development in Poland.

REFERENCES

- [1] D. Segala, P. Cavallaro, *Computational Materials Science* **81**, 303-312 (2014).
- [2] R. Panowicz, K. Sybilski, D. Kołodziejczyk, T. Niezgodą, W. Barnat, *Journal of KONES Powertrain and Transport* **18**, 4 (2011).
- [3] D.R. Possley, J.A. Blair, B.A. Freedman, A.J. Schoenfeld, R.A. Lehman, J.R. Hsu, *The Spine Journal* **12**, 843-848 (2012).
- [4] V.T. Inman, *The joints of the ankle*, 2nd ed., Baltimore: Williams & Wilkins; pp. 31-74, 1991.
- [5] J.R. Close, *J Bone Joint Surg Am* **38**, 761-81 (1956).
- [6] M.R. Colville, R.A. Marder, J.J. Boyle, B. Zarins, *Am. J. Sports Med.* **18**, 196-200., P. Renstrom, M. Wertz, S. Incavo, M. Pope, H.C. Ostgaard, (1990).
- [7] I.A. Kapandij, *The Physiology of the Joints*, Vol II, Churchill Livingstone, (1987).
- [8] D. Kent. Butz, D. Deva. Chan, A. Eric. Nauman, P. Corey, *Neu, Journal of Biomechanics* **44**, 15, 13, 2667-2672 October (2011).
- [9] D.L. France, *Human and nonhuman bone identification: a color atlas*. CRC Press, 2008.
- [10] J.T.M. Cheung, M. Zhang, *Finite element modeling of the human foot and footwear*. In: ABAQUS Users' Conference. p. 145-58 (2006).

- [11] J.M. Garcia-Aznar, J. Bayod, A. Rosas, R. Larrainzar, R. Garcia-Bogalo, M. Doblare, et al., *J Biomech Eng*, **131**:021011.R. (2009).
- [12] Y.T. Gu, Z.J. Yao, L.S. Jia, J. Qi, J. Wang, *Int Orthop*, **34**, 1251-9 (2010).
- [13] M.J. Sormaala, M.H. Niva, M.J. Kiuru, V.M. Mattila, H.K. Pihlajamaki, *Bone*, **39**:199-204(2006).
- [14] M.H. Niva, M.J. Sormaala, M.J. Kiuru, R. Haataja, J.A. Ahovuo, H.K. Pihlajamaki, *Am J Sports Med*, **35**:643-9(2007).
- [15] Y.C. Hsu, Y.W. Gung, S.L. Shih, C.K. Feng, S.H. Wei, C.H. Yu, et al. *Ann Biomed Eng*, **36**:1345-52(2008).
- [16] Tian-Xia Qiu, Ee-Chon Teo, Ya-Bo Yana, Wei Lei, *Medical Engineering & Physics* **33**, 1228-1233(2011).
- [17] J.R. Cho, S.B. Park, S.H. Kim, S.B. Lee, *J Mech Sci Technol*, **23**:2583-91(2009).
- [18] J.E. Bischof, C.E. Spritzer, A.M. Caputo, M.E. Easley, J.K. De Orio, J.A. Nunley, L.E. De Frate, *Journal of Biomechanics* **43**, 2561-2566(2010).
- [19] Can Xu, Ming-Yan Zhang, Guang-Hua Lei, Can Zhang, Shu-Guang Gao, Wen Ting, Kang-Hua Li, *Knee Surgery, Sports Traumatology, Arthroscopy*, September, **20**, 9, 1854-1862 (2012).
- [20] F. Wei, J.E. Braman., B.T. Weaver, R.C. Hautemal, *Journal of Biomechanics*, **44**, 15, 2636-2641, (2011).
- [21] P. Golano, J. Vega, P.A. de Leeuw, F. Malagelada, M.C. Manzanares, V. Gotzens V, C.N. van Dijk, *Knee Surg Sports Traumatol Arthrosc* **18**(5), 557-569 (2010).
- [22] C.W. Imhauser, S. Siegler, J.K. Udupa, J.R. Toy, *J Biomech* **41**(6), 1341-1349 (2008).
- [23] C.S. Mow, C.S. Proctor, M.A. Kelly, *Biomechanics of articular cartilage*. In: Nordin M, Frankle V (eds) *Basic biomechanics of the musculoskeletal system*. Lea and Febiger, Malvern PA, pp. 31-57 (1989).
- [24] S.D. Masouros, N. Newell, A. Ramasamy, T.J. Bonner, A.T.H. West, A.M. Hill, J.C. Clasper, A.M.J. Bull, *Annals of Biomedical Engineering* **41**, 9, 1957-1967 (2013).
- [25] T. Pandelani, D. Reinecke, F. Beetge, *Science real and relevant conference 2010*, Ref: DS04-PA-F, (2010).
- [26] M. Suresh, F. Zhu, K.H. Yang, J.L. Serres, R.E. Tannous, *Proceedings of the 10th World Congress on Computational Mechanics*, Sao Paulo, Brazil, (2012).
- [27] N. Newell, S.D. Masouros, A. Ramasamy, Bonner T.J., Hill A.M., Clasper J.M., Bull A MJ, *IRCOBI Conference* (2012).
- [28] K. Polak, M. Czyż, K. Ścigała, W. Jarmundowicz, R. Będziński, *Journal of the Mechanical Behavior of Biomedical Materials*, **34**, 165-170 (2014).
- [29] M. Czyż, K. Ścigała, R. Będziński, W. Jarmundowicz, *Acta of Bioengineering and Biomechanics* **14**, 4, 23-29 (2012).
- [30] R. Będziński, K. Ścigała, *STRAIN* (1999).
- [31] R. Będziński, K. Ścigała, *Computer Assisted Mechanics and Engineering Sciences* **10**, 353-368 (2003).
- [32] R. Będziński, *Biomechanika*, Instytut Podstawowych Problemów Techniki PAN, – (Mechanika Techniczna – Polska Akademia Nauk. Komitet Mechaniki; T. 12), red. R. Będziński – s. 21-75. – ISBN: 978-83-89687-61-6 (2011).
- [33] J. Shanti, M.K. Patil, *Journal of Rehabilitation Research & Development* **36**, 3, July (1999).
- [34] Suk-Hun Kim, Seung-Hwan Chang, Ho-Joong Jung, *Composite Structures* **92**, 2109-2118 (2010).
- [35] J.T. Cheung, M. Zhang, A.K. Leung, Y.B. Fan, *J Biomech*, **38**, 1045-54 (2005).

Received: 10 April 2015.